Nuclear Engineering and Technology 55 (2023) 2802–2811

Contents lists available at ScienceDirect

Nuclear Engineering and Technology

journal homepage: www.elsevier.com/locate/net

Original Article

Assessment of radionuclides from coal-fired brick kilns on the outskirts of Dhaka city and the consequent hazards on human health and the environment

M.M. Mahfuz Siraz [a], M.D.A. Rakib [b], M.S. Alam [b], Jubair Al Mahmud [b], Md Bazlar Rashid [c], Mayeen Uddin Khandaker [d, e], Md. Shafiqul Islam [b], S. Yeasmin [a, *]

[a] Health Physics Division, Atomic Energy Centre, Dhaka, 1000, Bangladesh
[b] Department of Nuclear Engineering, University of Dhaka, Dhaka, 1000, Bangladesh
[c] Geological Survey of Bangladesh, Segunbaghicha, Dhaka, 1000, Bangladesh
[d] Department of General Educational Development, Faculty of Science and Information Technology, Daffodil International University, DIU Rd, Dhaka, 1341, Bangladesh
[e] Centre for Applied Physics and Radiation Technologies, School of Engineering and Technology, Sunway University, 47500, Bandar Sunway, Selangor, Malaysia

A R T I C L E I N F O

Article history:
Received 8 January 2023
Received in revised form
29 March 2023
Accepted 29 April 2023
Available online 5 May 2023

Keywords:
Brick kilns
Soil
Radioactivity
Health hazards
HPGe Detector
Dhaka

A B S T R A C T

In a first-of-its-kind study, terrestrial radionuclide concentrations were measured in 35 topsoil samples from the outskirts of Dhaka using HPGe gamma-ray spectrometry to assess the radiological consequences of such a vast number of brick kilns on the plant workers, general as well as dwelling environment. The range of activity concentrations of ^{226}Ra, ^{232}Th, and ^{40}K is found at 19 ± 3.04 to 38 ± 4.94, 39 ± 5.85 to 57 ± 7.41, and (430 ± 51.60 to 570 ± 68.40) Bq/kg, respectively. ^{232}Th and ^{40}K concentrations were higher than the global averages. Bottom ash deposition in lowlands, fly ash buildup in soils, and the fallout of micro-particles are all probable causes of the elevated radioactivity levels. ^{137}Cs was found in the sample, which indicates the migration of ^{137}Cs from nuclear accidents or nuclear fallout, or the contamination of feed coal. Although the effective dose received by the general public was below the recommended dose limit but, most estimates of hazard parameters surpass their respective population weighted global averages, indicating that brick kiln workers and nearby residents are not safe due to prolonged exposures to terrestrial radiation. In addition, the soil around sampling sites is found to be unsuitable for agricultural purposes.

1. Introduction

Naturally occurring radioactive materials (NORMs), such as ^{232}Th, ^{226}Ra, and ^{40}K, which have the potential to cause radiotoxicity, can be found in various amounts in the organic and inorganic mineral aggregates of coal, a sedimentary rock [1–7]. Following the coal combustion in the brick kiln, the radioactive particles together with fly ash are released into the air and deposited onto the environment matrix (e.g., soil, water, plants, and atmosphere), hence they are redistributed and contributed to the elevated radiation concentrations of NORMs in the environment [8]. The radioactive load on the surrounding atmosphere could be significantly increased by the influence of these NORMs [2,9–11]. Fly ash is noticeably smaller in size than bottom ash. The concentration of natural radionuclides in fly ash is also significantly higher than that of bottom ash as well as feed coal [12]. Fly ash would therefore be categorized as a TENROM (technologically enhanced naturally occurring radioactive material), potentially posing a health danger to both brick kiln workers and the neighborhood at large [13].

Coal is used for baking bricks in kilns, which is known for producing complete and incomplete combustion products that are carcinogenic, genotoxic, cytotoxic, fibrogenic, and produce free radicals that damage DNA [14]. Radiation exposure can lead to a variety of problems, including diffuse alveolitis, fibrosis, DNA strand breakage, genetic mutations, and radiation pneumonitis. Black-lung disease is a common condition among coal burners

* Corresponding author.
E-mail address: selinayeasmin@yahoo.com (S. Yeasmin).

https://doi.org/10.1016/j.net.2023.04.045

because of the excessive amounts of inhaled coal dust [15,16]. Furthermore, exposure to coal's external gamma rays has been linked to an elevated risk of cancer in both coal miners and the local population living nearby; therefore, people who live close to the coal-fired brick kilns may have analogous impacts [17–19]. When compared to the control groups, it was shown that brick kiln workers had poor lung function, increased oxidative stress, increased DNA damage, and a rise in DNA-protein crosslinks (DPC) [14,20,21].

Fly ash from the chimney drifts to nearby farmland. Radionuclides (RNs) and toxic heavy metals are deposited into the environment (e.g., soil, water, plants, and atmosphere) together with fly ash in the form of harmful fumes, smoke, etc. Naturally Occurring Radioactive Materials (NORMs), which are typically found at varied trace levels in all geomaterials, are the primary external source of radiation for humans [22]. As a consequence of the deposition of fly ash in the surrounding soil and agricultural land, the levels of these NORMs are raised, and they are transferred from the soil to water sources and the food chain [23]. In order to assess potential changes in environmental radioactivity caused by activities like burning coal as fuel in brick kilns, it is crucial to identify, quantify, and characterize the radioactivity level, effective dose consequences, adverse effects, potential radiological risk, and distribution, accumulation, relocation, and origin of NORMs in soils [2,24,25]. Additionally, the presence of manmade radionuclides in the soil around brick kilns may be a sign that the feed coal used to bake the bricks was contaminated.

Bangladesh is situated on the deltas of numerous important rivers that flow into the Bay of Bengal. Due to the nation's location on an alluvial plain and the limited availability of natural rock for use in construction, bricks are the primary building material. Bricks are used both directly and after being broken down into coarse aggregate for the purpose of creating concrete. To accommodate this need, Bangladesh has about 7000 coal-fired brick kilns running, producing about 23 billion bricks annually. More than 1000 of them are located around the Dhaka megacity, the capital of the country [26,27]. In Bangladesh, coal is the main fuel used in the production of bricks consuming in excess of one million tons of coal per year [26]. Low-grade, high-sulfur coals supplied from India are frequently used in coal-fired brick kilns, and consequently, they unfortunately have negative impacts on human health and the environment on a global and regional scale [19].

A survey of literature shows the existence of several earlier studies on radioactivity in soil near the coal-fired power plants around the world. The maximum radioactive concentration was found in soil samples taken from places that were closest to the coal-fired power plant (CFPP) near the Tarn Taran region of Punjab, India (Dhingra et al., 2020). As the distance from the power plant increases, the concentrations of NORMs decrease. This pattern suggests that radioactivity has grown due to the accumulation of fly ash close to CFPP. Similar outcomes were reported in Figueira (Brazil) [28]; Cayirhan lignite CFPP, Ankara, Turkey [29]. Papaefthymiou et al. reported no discernible increase in radioactivity near a CFPP in Greece [30]. In soil samples from Turkey's Afsin-Elbistan coal-fired thermal power stations, high amount of the artificial radionuclide ^{137}Cs was detected [31]. A higher concentration of NORMs than the world average background radioactivity were found in the area surrounding the Barapukuria CFPP in Bangladesh [11]. No studies on radioactivity in soils around brick kilns near Dhaka megacity, have been found in the literature, however one study was undertaken in the south of Bangladesh and found decreasing radioactivity in all directions [19].

The purpose of this investigation, which is the first of its kind, is to determine how the operation of such a large number of brick kilns affects the radioactivity levels in soils and agricultural land around the kilns. Another purpose is to evaluate the relevant radiological hazard parameters to determine the associated radiation risks to nearby residents and workers, in light of the data available in the literature and the numerous brick kilns that can be found at the outskirts of the Dhaka megacity.

2. Methodology

2.1. Study area

The present study area is located in the central part of Bangladesh as shown in Fig. 1. Geologically, it is divided into the Madhupur clay deposit, alluvial valley fill deposit, marsh clay and pet deposit, and alluvial silt and clay deposit [32]. It consists of mainly plain land and Pleistocene alluvial terraces and composes of generally silt and clay. The Dhaleswar, Buriganga, Turag and Balu are the main rivers in the area. Due to the high demand of bricks in the capital city and its surrounding areas, so many brickfields are operated in this area.

2.2. Geological map preparation

Landsat satellite image of 2018 was collected from http://glovis.usgs.gov and employed in this study. The layer stack of the image was performed by Erdas Imagine 2014 software. The visual image investigation was carried out by ArcMap 10.2 to define the various geological units of the area (Fig. 1) as well as subsequent field checking according to our earlier research [33–35]. The geological map of Bangladesh [32] was also used to revalidate the map units.

2.3. Sample collection and preparation procedures

Thirty-five soil samples were collected around thirty-five brick kilns located at Savar, Dhamrai and Narayanganj. Seventeen soil samples (Sample no. 1–17) were collected from Madanpur, Bandar, Narayanganj; ten soil samples (Sample no. 18–27) were collected from Kalampur, Dhamrai, Dhaka; six soil samples (Sample no. 28–33) were collected from Bongaon, Savar, Dhaka; and two soil samples (Sample no. 34–35) were collected from Mograkanda, Savar, Dhaka following the systematic random sampling technique given in the IAEA guideline [36]. The samples were collected down to a depth of 10 cm in January 2022. After removing extraneous components like roots, pebbles, and plant matter, along with other impurities, the samples were thoroughly mixed. Each sample, weighing about 1 kg, then immediately stored in airtight, clean ziplock polyethene bags, adequately labeled. The samples were transported to the sample preparation room of the Health Physics Division of Atomic Energy Centre Dhaka (AECD) for further processing. The samples were homogenized, weighed, and dried to reduce moisture content in a temperature-controlled furnace. All samples were then put into radon-impermeable, airtight plastic cans after being crushed and powdered. Then they were kept for at least 40 days to reach secular equilibrium between the yields of the radioactive elements ^{222}Rn (^{226}Ra), ^{220}Rn (^{224}Ra), and their transient daughter elements. Cross-contamination was carefully avoided throughout sample preparation, measurement, and sampling [37].

2.4. Measurement procedures

Using a high-resolution coaxial HPGe gamma-ray spectrometer and the related electronics, the activity concentrations of gamma-ray-releasing radionuclides within the samples were determined. The detector was contained in a cylindrical lead shielding device

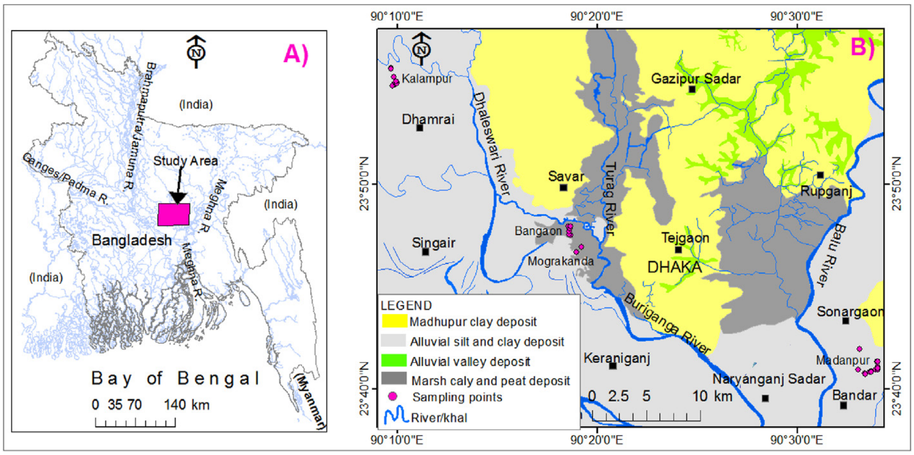

Fig. 1. A) Bangladesh, its surroundings and study area B) General geology of the study area and sampling points.

with a sliding cover and a fixed bottom to reduce noise interference from the environment. With a relative efficiency of 30%, it was found that the energy resolution of the 1.33 MeV energy peak for ^{60}Co was 1.69 keV at full-width half-maximum (FWHM).

2.5. Energy and efficiency calibration

The accuracy of the measured data largely depends on the energy and efficiency calibration of the detector, which must be carried out with extreme care. The detector's energy calibration was performed using common point sources like ^{22}Na, ^{57}Co, ^{60}Co, ^{133}Ba, ^{137}Cs, etc. A standard source was made by combining ^{152}Eu of known activity with the Al_2O_3 matrix and manufactured in the same containers as the samples to determine the detector efficiency.

2.6. Calculation of radioactivity

Using the characteristic gamma lines of 241.98 keV, 295.21 keV, and 351.92 keV for ^{214}Pb and 609 keV, 1120.3 keV and 1764.5 keV for ^{214}Bi, the activity concentration of ^{226}Ra was estimated. Conversely, the characteristic gamma lines 583.14 keV for ^{208}Tl, 911.07 keV and 969.11 keV for ^{228}Ac, were used to determine the ^{232}Th activity concentration [38,39]. Using the unique 1460.75 keV gamma line, which only occurs individually, the radioactivity of ^{40}K was estimated. The following Eq. (1) [40] was used to determine the radionuclide's activity concentration:

$$A_i = \frac{cps}{\varepsilon \times \rho_\gamma \times w} \tag{1}$$

Here, A_i is the specific activity in Bqkg^{-1}, *cps* is the count rate, ε is the HPGe detector's counting efficiency at the specific gamma-ray energy, ρ_γ represents the gamma-ray emission probability, and w is the sample weight in kilograms (kg). The minimal detectable activity concentration (MDAC) for the gamma-ray measurement system method was calculated using Eq. (2) as stated in Ref. [37]:

$$MDA = \frac{K_\alpha \times \sqrt{B}}{\varepsilon \times \rho_\gamma \times T \times w} \tag{2}$$

where K is the statistical coverage factor, with a value of 1.64 (at the 95% confidence level), B is the background counts for the relevant radionuclide, T is the counting time, ρ_γ represents the gamma-ray emission probability, and w is the sample weight in kilograms (kg). The MDAs for ^{226}Ra, ^{232}Th, and ^{40}K were determined to be 0.35 Bq/kg, 0.64 Bq/kg, and 2.2 Bq/kg, respectively.

Using the uncertainty propagation law of the relevant quantities represented in Eq. (2), the uncertainty of the measured radioactivity was determined. Eq. (3) expressed the mathematical formulation for calculating the uncertainty of the determined radioactivity [41,42].

$$\text{Combined Standard Uncertainty} = A_i \times \sqrt{\left(\frac{u(N)}{N}\right)^2 + \left(\frac{u(T)}{T}\right)^2 + \left(\frac{u(\rho_\gamma)}{\rho_\gamma}\right)^2 + \left(\frac{u(w)}{w}\right)^2 + \left(\frac{u(\varepsilon)}{\varepsilon}\right)^2} \tag{3}$$

The sample counts, counting time, gamma-ray emission probability, sample weight, and counting efficiency are represented by the letters N, T, ρ_γ, w, and ε, respectively. The calculated uncertainty of the relevant radionuclides varies about 10%.

2.7. Radiological hazard parameters

2.7.1. Radium equivalent activity

Non-uniform radioactivity in a material containing Ra, Th, and K can be modeled using the commonly used 'radium equivalent activity (Ra_{eq})' index, which represents the specific activities of ^{226}Ra, ^{232}Th, and ^{40}K in a single quantity while accounting for the radiation risks associated with each of these. The Ra_{eq} was determined using Eq. (4) to compare the combined radiological effect of ^{226}Ra, ^{232}Th, and ^{40}K in the materials [43,44]. For safe use, the maximum Ra_{eq} value must be lower than 370 Bq/kg.

$$Ra_{eq} = A_{Ra} + 1.43A_{Th} + 0.077A_K \tag{4}$$

Where, A_{Ra}, A_{Th}, and A_K represent the mean specific activities of ^{226}Ra, ^{232}Th, and ^{40}K in Bq/kg, respectively.

2.7.2. The absorbed dose rate in the air

The external absorbed dose rate, D_{out}, due to the exposure to the released gamma rays from the studied material at 1 m above the ground was calculated using the following Eq. (5)

$$D_{out} = 0.427A_{Ra} + 0.662A_{Th} + 0.0432A_K \tag{5}$$

D_{out} represents the outside absorbed dose rate in (nGy/h) owing to gamma-ray exposure, while the other symbols have their usual meaning. Furthermore, because earth crust-derived materials such as brick, sand, cement, paints, tiles, and so on are commonly used to construct dwellings, monitoring indoor exposure is crucial. Therefore, Eq. (6) is used to calculate it [45,46].

$$D_{in} = 1.4D_{out} \tag{6}$$

2.7.3. The annual effective dose

The annual effective doses of E_{in} and E_{out} can be calculated using the measured indoor and outdoor exposures, respectively. By using Eqs. (7) and (8), the annual effective doses E_{in} (mSv/y) and E_{out} (mSv/y) were calculated [22,47].

$$E_{in}\left(mSv/_{y}\right) = D_{in}\left(nGy/_{h}\right) \times \left(8760\ h/_{y} \times 0.7\ Sv/_{Gy} \times 0.8\right) \times 10^{-6} \tag{7}$$

$$E_{out}\left(mSv/_{y}\right) = D_{out}\left(nGy/_{h}\right) \times \left(8760\ h/_{y} \times 0.7\ Sv/_{Gy} \times 0.2\right) \times 10^{-6} \tag{8}$$

2.7.4. External hazard (H_{ex}) and internal hazard (H_{in}) indices

Using the external and internal hazard indices, the permissible equivalent dose should be lined up with a restricted value. For example, building materials should have a value of H_{ex} that is less than or equal to unity to reduce the radiation dosage [37]. By using Eq. (9) external hazard index (H_{ex}) can be calculated [48,49].

$$H_{ex} = \frac{A_{Ra}}{370} + \frac{A_{Th}}{259} + \frac{A_K}{4810} \tag{9}$$

Regarding the internal health risk brought on by radon exposure and the accumulation of its transient offspring on lung tissues, a quantitative index (H_{in}) known as the internal hazard index is provided by Eq. (10) [47,50].

$$H_{in} = \frac{A_{Ra}}{185} + \frac{A_{Th}}{259} + \frac{A_K}{4810} \tag{10}$$

2.7.5. Excess lifetime cancer risk (ELCR)

In the present study, the increased lifetime cancer risk related to the use of soil was calculated using the following Eq. (11) [51,52].

$$ELCR = E_{aed} \times A_{lf} \times R_f \tag{11}$$

E_{aed}, A_{lf}, and R_f represent the equivalent annual effective dosage, the average lifespan (72.6 years) [53] and the fatal-cancer risk factor, respectively. As the risk factor for stochastic impacts, ICRP report 60 recommends a value of 0.05 per Sievert for the general public [43].

2.7.6. Gamma level index (I_γ)

The representative level index can assess the degree of radiation

Table 1
Radioactivity of ^{226}Ra, ^{232}Th and ^{40}K in soil samples collected from thirty-five brick kilns.

Sample	Name of the brick company	Latitude (N)	-Longitude (E)	Activity Concentration (Bq/kg)		
				^{226}Ra	^{232}Th	^{40}K
01	Bismillah (909) bricks	23°40′41.9″	90°33′26.3″	28 ± 3.64	45 ± 4.50	470 ± 56.4
02	SKB bricks	23°40′43.2″	90°33′25.2″	24 ± 3.36	44 ± 6.60	450 ± 54
03	KBM bricks	23°40′47.7″	90°33′39.7″	38 ± 4.94	45 ± 6.75	440 ± 52.80
04	Ananda bricks	23°40′50.0″	90°33′42.4″	28 ± 3.64	41 ± 6.15	470 ± 56.40
05	Tata bricks	23°40′48.6″	90°33′43.0″	28 ± 3.64	42 ± 6.72	490 ± 58.80
06	MAB bricks	23°40′54.3″	90°33′55.8″	30 ± 3.90	44 ± 5.28	490 ± 58.80
07	505 bricks	23°40′54.5″	90°33′03.5″	31 ± 4.03	46 ± 6.44	480 ± 57.60
08	BRB bricks	23°41′57.0″	90°33′98.0″	32 ± 4.16	49 ± 7.35	490 ± 58.80
09	BBM bricks	23°41′03.5″	90°34′01.9″	33 ± 4.29	47 ± 6.58	470 ± 56.40
10	MBC bricks	23°40′55.2″	90°34′02.2″	29 ± 3.77	44 ± 7.04	510 ± 61.20
11	707 bricks	23°40′55.2″	90°34′03.4″	33 ± 4.29	42 ± 6.30	460 ± 55.20
12	Rupa bricks	23°41′00.5″	90°34′03.6″	38 ± 4.94	47 ± 7.05	440 ± 52.80
13	NBN bricks	23°41′20.1″	90°34′01.3″	19 ± 3.04	39 ± 5.85	430 ± 51.60
14	DBC bricks	23°41′20.1″	90°34′00.7″	36 ± 4.68	41 ± 6.56	430 ± 51.60
15	ABC bricks	23°41′18.9″	90°34′03.6″	31 ± 4.03	42 ± 6.72	440 ± 52.80
16	Bismillah (909) bricks	23°40′44.6″	90°33′23.0″	32 ± 4.48	57 ± 7.41	590 ± 70.80
17	2SB bricks	23°40′42.1″	90°33′26.0″	30 ± 3.90	41 ± 6.56	500 ± 60
18	MEBC bricks	23°54′54.3″	90°09′53.8″	29 ± 3.77	44 ± 6.16	460 ± 55.20
19	AB bricks	23°54′54.0″	90°09′49.2″	27 ± 3.51	45 ± 6.75	480 ± 57.60
20	MSBC bricks	23°55′42.3″	90°09′40.1″	26 ± 3.38	46 ± 6.44	500 ± 60
21	STIN bricks	23°54′51.0″	90°09′45.1″	29 ± 3.77	47 ± 4.23	480 ± 57.60
22	BBC bricks	23°55′02.5″	90°09′58.8″	30 ± 3.90	47 ± 7.05	500 ± 60
23	AHK bricks	23°54′59.7″	90°09′53.9″	34 ± 4.42	47 ± 7.05	510 ± 61.20
24	MLAB bricks	23°55′41.6″	90°09′41.8″	32 ± 4.16	48 ± 7.68	510 ± 61.20
25	MCBC bricks	23°54′56.1″	90°09′58.4″	31 ± 4.03	51 ± 5.10	570 ± 68.40
26	SUN bricks	23°55′02.6″	90°09′55.6″	29 ± 4.06	47 ± 6.58	520 ± 62.40
27	USA bricks	23°55′17.3″	90°09′49.2″	33 ± 4.29	49 ± 7.35	570 ± 68.40
28	City bricks	23°47′31.8″	90°18′40.4″	31 ± 4.03	48 ± 6.24	550 ± 60.50
29	AIM bricks	23°47′33.4″	90°18′36.7″	27 ± 3.51	45 ± 6.40	480 ± 57.60
30	Shapla bricks	23°47′56.3″	90°18′34.8″	30 ± 3.90	49 ± 7.84	520 ± 62.40
31	KBC bricks	23°47′42.3″	90°18′35.4″	31 ± 4.03	44 ± 6.16	510 ± 61.12
32	MIN bricks	23°47′50.5″	90°18′38.7″	27 ± 3.51	41 ± 6.15	500 ± 60
33	Shahin bricks	23°47′57.5″	90°18′39.5″	26 ± 3.38	40 ± 6	480 ± 57.60
34	SBB bricks	23°46′55.6″	90°19′12.7″	29 ± 3.77	42 ± 5.88	540 ± 64.80
35	SANY bricks	23°46′41.2″	90°18′57.0″	28 ± 3.64	42 ± 6.30	480 ± 57.60
Average				30 ± 3.69	45 ± 6.25	492 ± 55.49
Range				19 ± 3.04–38 ± 4.94	39 ± 5.85–57 ± 7.41	430 ± 51.60–570 ± 68.40

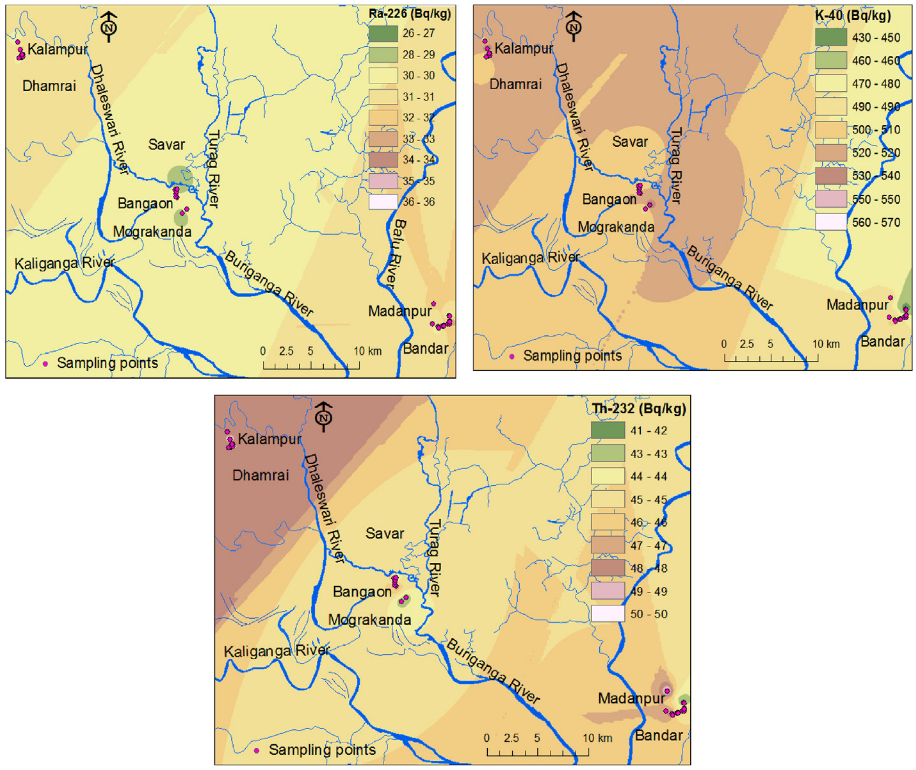

Fig. 2. Maps showing the distribution of the ^{226}Ra, ^{232}Th, and ^{40}K in soil samples collected around brick kilns.

risk associated with natural emitters in the soil. In addition, this index, which correlates the annual dose rate with excess radiation from surface materials, can be used as a screening tool for identifying materials used as building materials. Eq. (12) calculates the gamma level index [43].

$$I_\gamma = \frac{A_{Ra}}{150} + \frac{A_{Th}}{100} + \frac{A_K}{1500} \quad (12)$$

2.8. Spatial distribution of different parameters

To scrutinize the spatial distribution of various parameters (Fig. 1), GIS (Geographic Information System) mapping and interpolation were carried out using ArcGIS 10.2 software. The inverse distance weighting (IDW) technique was used to interpolate the value of a variable at unmeasured sites from observations of its values at nearby locations, according to our previous study [54,55].

3. Results and discussion

Table 1 shows the radioactivity concentrations of ^{40}K, ^{232}Th, and ^{226}Ra in the measured soil samples collected from thirty-five brick kilns. It is reported in Table 1 that all the values of ^{40}K, ^{232}Th, and most of the values of ^{226}Ra are higher than the world average values of 400, 35, and 30 Bqkg^{-1} for ^{40}K, ^{232}Th and ^{226}Ra, respectively [22]. There are distinct geological and topographical characteristics in every region of the world that influence soil radioactivity [56–60]. The modification of particular activities based on the types of rocks that resulted in the formation of soil. Igneous rocks like granite have higher radiation levels than sedimentary rocks [56,61–65]. The mobility of the radionuclides is also greatly influenced by their chemical characteristics. Along with geology, other factors that can affect the distribution of radionuclides in soil include regional geological events, the soil-to-water ratio, the site's latitude and altitude, industrial wastes, the use of pesticides and fertilizers, the processing of minerals, the treatment of water, the use of fossil fuels, the rate and amount of rainfall, soil drainage, site characteristics, and natural occurrences like earthquakes and forest fires [66,67]. The current investigation found that the measured activity of ^{40}K was significantly higher than that of ^{232}Th and ^{226}Ra because: (i) ^{40}K is the radioactive element that occurs most frequently in the environment, (ii) increasing agricultural yield by using chemical fertilizers (NPK, TSP, and SSP) (iii) coal burning produces several volatile K compounds [19,68,69]. The following are some potential causes of the increased activity near the brick kiln: (1) Fly ash deposition from the brick kiln elevated the natural radionuclide concentrations over the baseline level. During the brick-making season, the wind blows strongly in the direction of sampling, so fly ash typically discharges into the arable area surrounding the kiln, (2) Bottom ash produced by coal-fired brick kilns may be dumped on the nearby lowlands, (3) Following combustion, the mineral composition of coal may be absorbed by fine particles that may suspend in the air environment or deposit in the nearby soil. The spatial distribution of ^{226}Ra, ^{232}Th and ^{40}K of soil samples is shown in Fig. 2.

A noteworthy finding of the current investigation is the identification of the anthropogenic radionuclide ^{137}Cs in the soil sample. ^{137}Cs (3.3 ± 0.69 Bq/kg) was found in soil sample no. 26 (23°55′02.6″ N, 90°09′55.6″ E) collected around Sun Bricks in Kalampur, Dhamrai, Dhaka. The radioisotope ^{137}Cs discovered in this investigation was most likely created by - i) accidents at nuclear power plants (like the Fukushima and Chernobyl NPP tragedies), ii) perhaps due to atmospheric nuclear weapon testing by neighboring nations, India, China and Pakistan, iii) The coal used for burning could have been exposed to ^{137}Cs in some way (during mining or storage). The ^{137}Cs discovered in this study are lower

Table 2
Radioactivity in soil samples taken nearby the CFPP from different countries.

Sl	Location of the CFPP			Activity concentration (Bq/kg)				Reference
				^{226}Ra	^{232}Th	^{40}K	^{137}Cs	
				Range (Average)	Range (Average)	Range (Average)	Range(Average)	
1	CFPP in Tarn Taran district, Punjab, India	<1 km from CFPP	30.7 ± 5.5 –34.8 ± 6.0 (33.6 ± 1.9)	39.7 ± 5.6–54.8 ± 7.1 (45.9 ± 6.4)	143 ± 103–324 ± 115 (233 ± 75.6)			[71]
		1–3 km from CFPP	27.0 ± 5.3 –29.8 ± 5.4 (28.2 ± 0.8)	37.6 ± 5.4–45.7 ± 6.1 (40.9 ± 2.1)	252.8 ± 38.9 (200 ± 103–306 ± 108)			
		3–5 km from CFPP	20.3 ± 4.8 –26.8 ± 5.2 (23.9 ± 2.2)	33 ± 5.1–41.9 ± 5.8 (38.4 ± 3.7)	181.3 ± 95.9 –273 ± 105 (219.7 ± 45.8)			
2.	CFPP, Figueira, Brazil	0–25 cm	<1 km	81±1–270 ± 3 (133 ± 59)	18±1–51 ± 2 (39 ± 9)	120 ± 13–412 ± 19 (233 ± 96)		[28]
			1 km	18±1–84 ± 1 (50 ± 22)	14±1–40 ± 1 (31 ± 10)	93 ± 10–225 ± 120.8 (190 ± 56)		
			3 km	29±1–72 ± 1(39 ± 15)	21±1–51 ± 1 (30 ± 10)	55 ± 11–328 ± 15 (161 ± 90)		
		25–50 cm	<1 km	16±1–154 ± 2 (71 ± 38)	24±1–55 ± 2 (40 ± 11)	138 ± 12–259 ± 12 (178 ± 55)		
			1 km	15±1–69 ± 1 (44 ± 18)	13±1–59 ± 1 (35 ± 16)	74±9–291 ± 12 (182 ± 60)		
			3 km	20±1–52 ± 1 (36 ± 11)	<8–58 ± 1 (30 ± 21)	<59–289 ± 15 (161 ± 102)		
3.	Cayirhan lignite CFPP, Ankara, Turkey	Within CFPP		(47.00 ± 2.45)	(32.54 ± 4.75)	(646.29 ± 32.30)		[29]
		4 km south of the CFPP		(28.16 ± 1.69)	(25.88 ± 3.2)	(371.73 ± 26.90)		
4.	West of Kapar, Malaysia	Near to the power plant		79.57 ± 7.1–92.27 ± 8.9 (86.7)	69.67 ± 5.9 –83.77 ± 7.59(74.3)	263.17 ± 21.7 –311.37 ± 28.3 (297.3)		[13]
		Near CPP and Garbage dumping area		100.57 ± 8.9 –152.87 ± 10.2 (120.7)	61.37 ± 5.9 –77.27 ± 6.6 (67.5)	305.57 ± 26.9 –392.57 ± 32.7(347.9)		
		Near CPP		49.67 ± 5.0–71.27 ± 6.9 (58.0)	37.47 ± 4.1 –56.87 ± 5.6 (51.3)	262.57 ± 22.3 –358.2 ± 30.0 (320.1)		
		Inside Kapar town		65.47 ± 6.2–68.57 ± 6.3 (67.3)	35.67 ± 3.3 –53.57 ± 5.1 (44.4)	274.6 ± 22.7 –314.4 ± 26.1 (296.7)		
5.	Afsin-Elbistan coal-fired thermal power plants, Turkey			5.8 ± 0.4–71.3 ± 3.7 (34.4)	5.4 ± 0.4–59.8 ± 3.3 (39.8)	138.6 ± 7.2–577.7 ± 29.5 (409.4)	9.5 ± 0.5 –239.7 ± 12.0 (50.5)	[31]
6.	Mawan CFPP, South China	<1 km		160-271 (225)	220-309 (257)	1125-2168 (1571)		[72]
		1–3 km		172-358(241)	135-298(215)	948-1762 (1265)		
		3–4 km		72-193(130)	117-432(321)	101-1367 (811)		
		Shenzhen Background, China		38-143 (91)	18-262(134)	54-1424 (417)		
7.	Lignite-fired power plants, Megalopolis Basin, Greece			21.5 ± 0.4–125 ± 3.2 (45.0 ± 2.5)	25.8 ± 0.2–40.2 ± 3.0 (32.5 ± 4.5)	228 ± 29–412 ± 28 (337 ± 58)	7.2 ± 0.6–314 ± 24 (80.5 ± 9.8)	[30]
8.	Brown CFPP, Ajka, Hungary			15.7 ± 2.4–883 ± 13 (129)	11.6 ± 2.6–43 ± 7 (26.9)	146 ± 23–596 ± 39 (337)	BDL-150 ± 14 (20.4)	[73]
9.	Coal Fired Brick Klin, Chattogram, Bangladesh			33.7 ± 10.9–54.3 ± 11.3 (45 ± 11.3)	44.2 ± 15.8 –62.1 ± 18.2 (51 ± 18.0)	307 ± 122–572 ± 123 (423 ± 122)		[19]
10.	Barapukuria CFPP, Dinajpur, Bangladesh			33-118(80.6)	43-182(104.4)	318.3–743.4 (508.1)		[2]
11	Southwestern part of Turkey	Yatagan CFPP		18-53 (32 ± 9)	17-89(37 ± 16)	23-794 (455 ± 165)	BDL-209	[74]
		Yenikoy and Kemerkoy CFPP		9-168 (42 ± 30)	6-74(32 ± 14)			
12	Catalagzi CFPP, west black sea coast, Turkey			(<1)-85.0 ± 9.2 (30.5 ± 21.2)	(<4)-67.5 ± 8.2 (39.7 ± 16.7)	128.9 ± 11.4 –691.1 ± 26.3 (378.7 ± 166.1)		[75]
13.	National Thermal Power Corporation (NTPC), Dadri (U.P) India,			32.2 ± 5.9 –120.9 ± 4.5(70.0 ± 8.9)	19.3 ± 0.9–44.6 ± 1.5(34.8 ± 1.2)	195.4 ± 2.8–505.4 ± 6.3 (436.1 ± 5.6)		[76]
14.	CFPP of Velilla, North of Spain			14-67 (39)	15-68 (43)	97-790 (445)		[77]
15.	Several coal-fired power plants in the Lodz region of Poland			8.8–22.6 (16.6 ± 0.9)	9.0–20.0 (15.7 ± 0.8)	221.5–434.2 (301.25)	0.6–14.9 (6.87)	[78]
16.	Baoji coal-fired power plant in China			12.54–40.18 (27.35)	38.02–72.55 (52.66)	498.02–1126.98 (764.27)		[79]
17.	Baqiao coal fired power plant in China			27.6–48.8 (36.1)	44.4–61.4 (51.1)	640.2–992.2 (733.9)		[80]
18.	Coal Fired Brick Klin, Savar, Dhamrai and Narayanganj, Bangladesh			19 ± 3.04–38 ± 4.94 (30 ± 3.69)	39 ± 5.85–57 ± 7.41 (45 ± 6.25)	430 ± 51.60–570 ± 68.40 (492 ± 55.49)	(3.3 ± 0.69)	Current study

than the 51 $Bqkg^{-1}$ global average value for ^{137}Cs given by UNSCEAR [22,70]. As a result, nearby peoples are not at risk for radiation exposure from such small quantities of ^{137}Cs.

Data on radioactivity in the soils surrounding a coal-fired brick kiln in Bangladesh or elsewhere are minimal, so we compare our results with the radioactivity in soil samples near coal-fired power plants (CFPP) around the world as shown in Table 2.

Soil samples collected from locations closest (1 km) to the CFPP near the Tarn Taran area of Punjab, India [71], have the highest radioactivity concentration and continue to decrease with distance from the power plant (1–3 km, 3–5 km). This pattern suggests an increase in radioactivity brought on by the accumulation of fly ash close to CFPP. Similar results were found in CFPP (<1 km, 1 km, 3 km of CFPP) in Figueira (Brazil) [28]; Cayirhan lignite CFPP (within

Table 3
Radiological hazard parameters in the soil samples used in this study.

Sl	Ra_{eq} $Bqkg^{-1}$	D_{out} $nGyhr^{-1}$	D_{in} $nGyhr^{-1}$	H_{ex}	H_{in}	E_{out} $mSvyr^{-1}$	E_{in} $mSvyr^{-1}$	E $mSvyr^{-1}$	I_γ	(ELCR) × 10^{-3}
01	128.54	62.05	74.46	0.35	0.42	0.08	0.37	0.44	0.95	0.28
02	121.57	58.82	70.58	0.33	0.39	0.07	0.35	0.42	0.90	0.26
03	136.23	65.02	78.03	0.37	0.47	0.08	0.38	0.46	1.00	0.29
04	122.82	59.40	71.28	0.33	0.41	0.07	0.35	0.42	0.91	0.27
05	125.79	60.93	73.11	0.34	0.42	0.07	0.36	0.43	0.93	0.27
06	130.65	63.11	75.73	0.35	0.43	0.08	0.37	0.45	0.97	0.28
07	133.74	64.43	77.31	0.36	0.45	0.08	0.38	0.46	0.99	0.29
08	139.80	67.27	80.72	0.38	0.46	0.08	0.40	0.48	1.03	0.30
09	136.40	65.51	78.61	0.37	0.46	0.08	0.39	0.47	1.00	0.29
10	131.19	63.54	76.25	0.35	0.43	0.08	0.37	0.45	0.97	0.28
11	128.48	61.77	74.12	0.35	0.44	0.08	0.36	0.44	0.95	0.28
12	139.09	66.35	79.62	0.38	0.48	0.08	0.39	0.47	1.02	0.30
13	107.88	52.51	63.01	0.29	0.34	0.06	0.31	0.37	0.80	0.23
14	127.74	61.09	73.31	0.35	0.44	0.07	0.36	0.43	0.94	0.27
15	124.94	60.05	72.06	0.34	0.42	0.07	0.35	0.43	0.92	0.27
16	158.94	76.89	92.26	0.43	0.52	0.09	0.45	0.55	1.18	0.34
17	127.13	61.55	73.86	0.34	0.42	0.08	0.36	0.44	0.94	0.27
18	127.34	61.38	73.66	0.34	0.42	0.08	0.36	0.44	0.94	0.27
19	128.31	62.06	74.47	0.35	0.42	0.08	0.37	0.44	0.95	0.28
20	130.28	63.15	75.78	0.35	0.42	0.08	0.37	0.45	0.97	0.28
21	133.17	64.23	77.08	0.36	0.44	0.08	0.38	0.46	0.98	0.29
22	135.71	65.52	78.63	0.37	0.45	0.08	0.39	0.47	1.00	0.29
23	140.48	67.66	81.20	0.38	0.47	0.08	0.40	0.48	1.04	0.30
24	139.91	67.47	80.97	0.38	0.46	0.08	0.40	0.48	1.03	0.30
25	147.82	71.62	85.95	0.40	0.48	0.09	0.42	0.51	1.10	0.32
26	136.25	65.96	79.15	0.37	0.45	0.08	0.39	0.47	1.01	0.29
27	146.96	71.15	85.38	0.40	0.49	0.09	0.42	0.51	1.09	0.32
28	141.99	68.77	82.53	0.38	0.47	0.08	0.40	0.49	1.05	0.31
29	128.31	62.06	74.47	0.35	0.42	0.08	0.37	0.44	0.95	0.28
30	140.11	67.71	81.25	0.38	0.46	0.08	0.40	0.48	1.04	0.30
31	133.19	64.40	77.28	0.36	0.44	0.08	0.38	0.46	0.99	0.29
32	124.13	60.27	72.33	0.34	0.41	0.07	0.35	0.43	0.92	0.27
33	120.16	58.32	69.98	0.32	0.39	0.07	0.34	0.41	0.89	0.26
34	130.64	63.52	76.22	0.35	0.43	0.08	0.37	0.45	0.97	0.28
35	125.02	60.50	72.60	0.34	0.41	0.07	0.36	0.43	0.93	0.27
Average	132.31	63.89	76.66	0.36	0.44	0.08	0.38	0.45	0.98	0.28
World Average [22]	370 [81]	59	84	<1	<1			1	<1	0.29

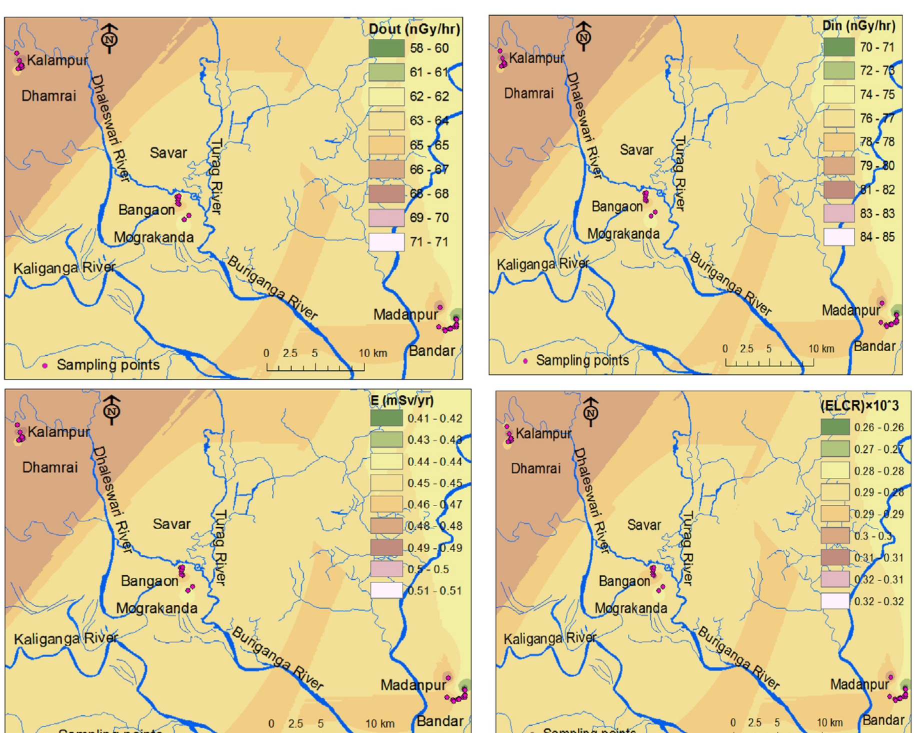

Fig. 3. The spatial distribution of outdoor and indoor absorbed dose rate, total effective dose and excess lifetime cancer risk.

CFPP, 4 km south of CFPP), Ankara, Turkey [29]; 2420 MW Sultan Salahuddin Abdul Aziz thermal CFPP in Malaysia [13].

Soil samples from Turkey's Afsin-Elbistan coal-fired thermal power station showed a shocking amount of the radioactive material ^{137}Cs [31]. The continental climate was cold, the sampling elevations were pretty high, and most of the winter was covered in snow. Therefore, excessive precipitation may cause increased ^{137}Cs levels in Elbistan. Forty-three sites in South China's Mawan CFPP were sampled for soil at distances of 1, 1–3, and 3–4 km [72]. The authors conclude that a combination of circumstances, including a greater concentration of natural radionuclides in fly ash and a high background radiation level, led to the high level of natural radionuclides in soils near Mawan CFPP. The highest activity concentrations of ^{226}Ra, ^{232}Th, and ^{40}K in soil samples collected from Bangladesh's Chattogram district at a distance of 120 m from agricultural soils next to a coal-fired brick kiln were discovered to be 54.3 ± 11.3 $Bqkg^{-1}$, 62.1 ± 18.2 $Bqkg^{-1}$, and 572 ± 123 $Bqkg^{-1}$, respectively [19]; the levels show a steady downward trend in every direction (towards and away from the kiln). Radioactivity of ^{226}Ra, ^{232}Th, and ^{40}K was significantly higher than the corresponding global average value in soil samples taken from the vicinity of the Barapukuria CFPP in Bangladesh [2].

The results of the present investigation (mean values of ^{226}Ra, ^{232}Th, and ^{40}K) are in close accordance with past worldwide studies, such as in CFPP in Tarn Taran district, Punjab, India [71]; Afsin-Elbistan coal-fired thermal power plants, Turkey [31]; Yatagan CFPP, Southwestern part of Turkey [74]; CFPP of Velilla, North of Spain [77]; Baqiao coal fired power plant in China [80]. Information on radiological hazard parameters is shown in Table 3.

All radium-equivalent activity values are much below the acceptable threshold of 370 $Bqkg^{-1}$ [81]. In addition, external and internal hazard indices for each sample were less than unity. The annual effective dose associated with soil samples under this study is less than the recommended dose limit of 1 mSv/y for the general public and 20 mSv/y for occupational workers [22]. However, most of the outdoor absorbed dose rate values, some indoor absorbed dose rate values, the gamma level index, and the excess lifetime cancer risk are higher than the corresponding global average values reported in Table 3. This data indicates that the area surrounding the majority of brick kilns is not radiologically safe for coal workers, who typically do not protect themselves from exposure to ash particles despite working long hours, and that the soil surrounding the brick kiln should not be used in building construction and agricultural purposes. Fig. 3 depicts the spatial distribution of several hazard characteristics.

4. Conclusion

This is the first attempt to determine radioactive levels and health hazard indices in brick kilns near the megacity of Dhaka. Thirty-five samples were collected from Savar, Dhamrai, and Narayanganj to evaluate radioactivity levels in brick kiln soil.

The mean activity concentrations ^{226}Ra, ^{232}Th and ^{40}K were 30 ± 3.69, 45 ± 6.25 and 492 ± 55.49 Bq/kg, respectively. All of the ^{232}Th, ^{40}K, and some of the ^{226}Ra values in this study exceeded the global averages of 35, 400, and 30 Bq/kg for ^{232}Th, ^{40}K, and ^{226}Ra, respectively. Fly ash deposition, bottom ash dumping in the nearby fields, and excessive usage of fertilizers were the primary reasons behind the elevated activity concentration of radionuclides.

All measures of radium-equivalent activity are well below the recommended limit. In addition, the internal and external hazard index values for each sample were below unity. Nonetheless, gamma level index, and excess lifetime cancer risk values are above the corresponding global average values, as do most outdoor and indoor absorbed dose rate values. The annual effective dosage associated with the studied soil samples is less than the recommended exposure limits of 1 mSv/y for the general population and 20 mSv/y for occupational workers.

Considering that most long-term coal miners do not use protective gear while exposed to ash particles, we may assume that the area under consideration is not radiologically safe. In addition, we may conclude that the land surrounding the kiln cannot be used for agriculture or manufacturing building materials.

5. Recommendations

- It is necessary to conduct monitoring on a consistent and exhaustive basis of the radioactivity of soil around Dhaka.
- The management of fly ash discharge should be significantly improved, and the exposure of locals to radiation should be reduced as much as possible.
- The transfer factor from soil to various crops must be calculated by studying water, food, and grass samples around the brick kiln.
- The health and safety of employees who have worked in the kiln for an extended time must be monitored periodically.
- Since no research on brick kilns has been conducted outside of Dhaka, investigating additional areas of Bangladesh with a significant concentration of brick kilns is urgently required.

Funding

This research did not receive any specific grant from funding agencies in the public, commercial, or not-for-profit sectors.

Author contributions

All authors contributed to the study's conception and design. [Mir Dider Ali Rakib] performed sample collection. [Dr. Md. Bazlar Rashid] was responsible for the geological analysis of the study area and drew the geological and radiological maps included in the manuscript. [Jubair Al Mahmud], [M.S. Alam], and [M.M. Mahfuz Siraz] performed the data analysis and prepared the first draft of the manuscript. The research was carried out under the keen supervision of [Dr. Md. Shafiqul Islam] and [S. Yeasmin], who performed the initial revisions of the first draft. [Dr. Mayeen Uddin Khandaker] performed the preliminary revisions of the first draft and provided important corrections & made the final revision and corrections. The final manuscript has been read and approved by all authors.

Consent of participation

No humans or experimental animals were subject to study in this particular research.

Data availability

On request, any and all data that was utilized in this study can be made available.

Declaration of competing interest

The authors declare that they have no known competing financial interests or personal relationships that could have appeared to influence the work reported in this paper.

References

[1] I. Akkurt, B. Mavi, H. Akyldrm, K. Gunoglu, Natural radioactivity of coals and

its risk assessment, Int. J. Phys. Sci. 4 (2009) 403–406, https://doi.org/10.5897/IJPS.9000391.
[2] M.A. Habib, R. Khan, K. Phoungthong, Evaluation of environmental radioactivity in soils around a coal burning power plant and a coal mining area in Barapukuria, Bangladesh: radiological risks assessment, Chem. Geol. 600 (2022), 120865, https://doi.org/10.1016/j.chemgeo.2022.120865.
[3] Ž. Vuković, M. Mandić, D. Vuković, Natural radioactivity of ground waters and soil in the vicinity of the ash repository of the coal-fired power plant "Nikola Tesla" A—obrenovac (Yugoslavia), J. Environ. Radioact. 33 (1996) 41–48, https://doi.org/10.1016/0265-931X(95)00067-K.
[4] S. Dragović, M. Ćujić, L. Slavković-Beškoski, B. Gajić, B. Bajat, M. Kilibarda, A. Onjia, Trace element distribution in surface soils from a coal burning power production area: a case study from the largest power plant site in Serbia, Catena 104 (2013) 288–296, https://doi.org/10.1016/J.CATENA.2012.12.004.
[5] J.A. Galhardi, R. García-Tenorio, D.M. Bonotto, I. Díaz Francés, J.G. Motta, Natural radionuclides in plants, soils and sediments affected by U-rich coal mining activities in Brazil, J. Environ. Radioact. 177 (2017) 37–47, https://doi.org/10.1016/J.JENVRAD.2017.06.001.
[6] A.M.A. Seid, Ş. Turhan, A. Kurnaz, T.K. Bakır, A. Hançerlioğulları, Radon concentration of different brands of bottled natural mineral water commercially sold in Turkey and radiological risk assessment, Int. J. Environ. Anal. Chem. 102 (2022) 7469–7481, https://doi.org/10.1080/03067319.2020.1830989.
[7] S. Turhan, Evaluation of agricultural soil radiotoxic element pollution around a lignite-burning thermal power plant, Radiochim. Acta 108 (2019) 77–85, https://doi.org/10.1515/RACT-2018-3051/MACHINEREADABLECITATION/RIS.
[8] E. Charro, V. Peña, Environmental impact of natural radionuclides from a coal-fired power plant in Spain, Radiat. Protect. Dosim. 153 (2013) 485–495, https://doi.org/10.1093/RPD/NCS126.
[9] F. Noli, P. Tsamos, S. Stoulos, Spatial and seasonal variation of radionuclides in soils and waters near a coal-fired power plant of Northern Greece: environmental dose assessment, J. Radioanal. Nucl. Chem. 311 (2017) 331–338, https://doi.org/10.1007/S10967-016-5082-0/METRICS.
[10] R. Khan, M.S. Parvez, U. Tamim, S. Das, M.A. Islam, K. Naher, M.H.R. Khan, F. Nahid, S.M. Hossain, Assessment of rare earth elements, Th and U profile of a site for a potential coal based power plant by instrumental neutron activation analysis, Radiochim. Acta 106 (2018) 515–524, https://doi.org/10.1515/RACT-2017-2867/MACHINEREADABLECITATION/RIS.
[11] M.A. Habib, T. Basuki, S. Miyashita, W. Bekelesi, S. Nakashima, K. Techato, R. Khan, A.B.K. Majlis, K. Phoungthong, Assessment of natural radioactivity in coals and coal combustion residues from a coal-based thermoelectric plant in Bangladesh: implications for radiological health hazards, Environ. Monit. Assess. 191 (2019) 27, https://doi.org/10.1007/s10661-018-7160-y.
[12] A.A. Sabuti, C.A.R. Mohamed, Activity levels of 210Po in the Coastal Area of Kapar, Malaysia, close to a coal-fired power plant, Sains Malays. 41 (2012) 815–828.
[13] Y.M. Amin, M. Uddin Khandaker, A.K.S. Shyen, R.H. Mahat, R.M. Nor, D.A. Bradley, Radionuclide emissions from a coal-fired power plant, Appl. Radiat. Isot. 80 (2013) 109–116, https://doi.org/10.1016/j.apradiso.2013.06.014.
[14] R. Kaushik, F. Khaliq, M. Subramaneyaan, R.S. Ahmed, Pulmonary dysfunctions, oxidative stress and DNA damage in brick kiln workers, Hum. Exp. Toxicol. 31 (2012) 1083–1091, https://doi.org/10.1177/0960327112450899.
[15] R.B. Finkelman, W. Orem, V. Castranova, C.A. Tatu, H.E. Belkin, B. Zheng, H.E. Lerch, S.V. Maharaj, A.L. Bates, Health impacts of coal and coal use: possible solutions, Int. J. Coal Geol. 50 (2002) 425–443, https://doi.org/10.1016/S0166-5162(02)00125-8.
[16] S. Buchanan, E. Burt, P. Orris, Beyond black lung: scientific evidence of health effects from coal use in electricity generation, J. Publ. Health Pol. 35 (2014) 266–277, https://doi.org/10.1057/jphp.2014.16.
[17] I. Demir, I. Kursun, Investigation of radioactive contents of Manisa-Soma and Istambul-Agacli coals (Turkey), Physicochem. Probl. Miner. Process. 48 (2012) 341–353, https://doi.org/10.5277/ppmp120202.
[18] M.E. Emirhan, C.S. Ozben, Assessment of radiological risk factors in the Zonguldak coal mines, Turkey, J. Radiol. Prot. 29 (2009) 527, https://doi.org/10.1088/0952-4746/29/4/007.
[19] M.J. Abedin, M.R. Karim, S. Hossain, N. Deb, M. Kamal, M.H.A. Miah, M.U. Khandaker, Spatial distribution of radionuclides in agricultural soil in the vicinity of a coal-fired brick kiln, Arabian J. Geosci. 12 (2019), https://doi.org/10.1007/s12517-019-4355-7.
[20] M. Khisroon, A. Khan, M. Imran, F. Zaidi, F. Ahmadullah, S.H. Fatima, Biomonitoring of DNA damage in individuals exposed to brick kiln pollution from Peshawar, Khyber Pakhtunkhwa, Pakistan, Arch. Environ. Occup. Health 73 (2018) 115–120, https://doi.org/10.1080/19338244.2017.1304881.
[21] R. Budhwar, V. Bihari, N. Mathur, A. Srivastava, S. Kumar, DNA-protein crosslinks as a biomarker of exposure to solar radiations: a preliminary study in brick-kiln workers, Biomarkers 8 (2003) 162–166, https://doi.org/10.1080/1354750031000067495.
[22] UNSCEAR, Sources and Effects of Ionizing Radiation Report to the General Assembly with Scientific Annexes, Annex-B, New York, 2000.
[23] B. Skoko, G. Marović, D. Babić, M. Šoštarić, M. Jukić, Plant uptake of 238U, 235U, 232Th, 226Ra, 210Pb and 40K from a coal ash and slag disposal site and control soil under field conditions: a preliminary study, J. Environ. Radioact. 172 (2017) 113–121, https://doi.org/10.1016/j.jenvrad.2017.03.011.
[24] M. Ćujić, S. Dragović, M. Đorđević, R. Dragović, B. Gajić, Š. Miljanić, Radionuclides in the soil around the largest coal-fired power plant in Serbia: radiological hazard, relationship with soil characteristics and spatial distribution, Environ. Sci. Pollut. Res. 22 (2015) 10317–10330, https://doi.org/10.1007/s11356-014-3888-2.
[25] A. Baeza, J.A. Corbacho, J. Guillén, A. Salas, J.C. Mora, B. Robles, D. Cancio, Enhancement of natural radionuclides in the surroundings of the four largest coal-fired power plants in Spain, J. Environ. Monit. 14 (2012) 1064–1072, https://doi.org/10.1039/C2EM10991C.
[26] G. DoE, National Strategy for Sustainable Brick Production in Bangladesh, 2017, p. 41. http://ccacoalition.org/sites/default/files/resources/2017_strategy-brick-production-bangladesh.pdf.
[27] S.E. Haque, M.M. Shahriar, N. Nahar, M.S. Haque, Impact of brick kiln emissions on soil quality: a case study of Ashulia brick kiln cluster, Bangladesh, Environ. Challenges. 9 (2022), 100640, https://doi.org/10.1016/J.ENVC.2022.100640.
[28] M. Flues, V. Moraes, B.P. Mazzilli, The influence of a coal-fired power plant operation on radionuclide concentrations in soil, J. Environ. Radioact. 63 (2002) 285–294, https://doi.org/10.1016/S0265-931X(02)00035-8.
[29] U. Cevik, N. Damla, S. Nezir, Radiological characterization of Cayirhan coal-fired power plant in Turkey, Fuel 86 (2007) 2509–2513, https://doi.org/10.1016/j.fuel.2007.02.013.
[30] H.V. Papaefthymiou, M. Manousakas, A. Fouskas, G. Siavalas, Spatial and vertical distribution and risk assessment of natural radionuclides in soils surrounding the lignite-fired power plants in megalopolis basin, Greece, Radiat. Protect. Dosim. 156 (2013) 49–58, https://doi.org/10.1093/rpd/nct037.
[31] A. Çayir, M. Belivermiş, Ö. Kiliç, M. Coşkun, M. Coşkun, Heavy metal and radionuclide levels in soil around Afsin-Elbistan coal-fired thermal power plants, Turkey, Environ. Earth Sci. 67 (2012) 1183–1190, https://doi.org/10.1007/s12665-012-1561-y.
[32] A. Al, G.S. of B. Alam, Md Khurshid, A.K.M. Shahidul Hasan, Mujibur Rahman Khan, John W. Whitney, S.K.M. Abdullah, James E. Queen, Geological Survey (U.S.), Office of Scientific Publications, Geological map of Bangladesh, Geological Survey of Bangladesh, 1990.
[33] M.B. Rashid, M.A. Habib, R. Khan, A.R.M.T. Islam, Land transform and its consequences due to the route change of the Brahmaputra River in Bangladesh, Int. J. River Basin Manag. 21 (2021) 1–13, https://doi.org/10.1080/15715124.2021.1938095.
[34] M.B. Rashid, Channel bar development and bankline migration of the Lower Padma River of Bangladesh, Arabian J. Geosci. 13 (2020) 612, https://doi.org/10.1007/s12517-020-05628-9.
[35] M.B. Rashid, M.A. Habib, Channel bar development, braiding and bankline migration of the Brahmaputra-Jamuna river, Bangladesh through RS and GIS techniques, Int. J. River Basin Manag. (2022) 1–13, https://doi.org/10.1080/15715124.2022.2118281.
[36] U. Barnekow, S. Fesenko, V. Kashparov, G. KisBenedek, G. Matisoff, Y. Onda, N. Sanzharova, S. Tarjan, A. Tyler, B. Varga, Guidelines on Soil and Vegetation Sampling for Radiological Monitoring Technical Reports Series No. 486, IAEA, Vienna, Austria, 2019.
[37] S. Amatullah, R. Rahman, J. Ferdous, M.M.M. Siraz, M.U. Khandaker, S.F. Mahal, Assessment of radiometric standard and potential health risks from building materials used in Bangladeshi dwellings, Int. J. Environ. Anal. Chem. (2021) 1–13, https://doi.org/10.1080/03067319.2021.1907361.
[38] International Atomic Energy Agency, Measurement of Radionuclides in Food and the Environment, Technical Reports Series No. 295, Vienna, Austria, 1989.
[39] M.S.D. Sarker, R. Rahman, M.M.M. Siraz, M.U. Khandaker, S. Yeasmin, The presence of primordial radionuclides in powdered milk and estimation of the concomitant ingestion dose, Radiat. Phys. Chem. 188 (2021), 109597, https://doi.org/10.1016/j.radphyschem.2021.109597.
[40] M.U. Khandaker, O.B. Uwatse, K.A. Bin Shamsul Khairi, M.R.I. Faruque, D.A. Bradley, Terrestrial radionuclides in surface (dam) water and concomitant dose in metropolitan Kuala Lumpur, Radiat. Protect. Dosim. 185 (2019) 343–350, https://doi.org/10.1093/RPD/NCZ018.
[41] K. Asaduzzaman, F. Mannan, M. Uddin Khandaker, M. Salihu Farook, A. Elkezza, Y. Bin Mohd Amin, S. Sharma, H. Bin Abu Kassim, Assessment of natural radioactivity levels and potential radiological risks of common building materials used in Bangladeshi dwellings, PLoS One 10 (2015), 140667, https://doi.org/10.1371/journal.pone.0140667.
[42] M.U. Khandaker, N. Adillah, B. Heffny, Y.M. Amin, D.A. Bradley, Elevated concentration of radioactive potassium in edible algae cultivated in Malaysian seas and estimation of ingestion dose to humans, Algal Res. 38 (2019), 101386, https://doi.org/10.1016/j.algal.2018.101386.
[43] M.U. Khandaker, K. Asaduzzaman, A.F. Bin Sulaiman, D.A. Bradley, M.O. Isinkaye, Elevated concentrations of naturally occurring radionuclides in heavy mineral-rich beach sands of Langkawi Island, Malaysia, Mar. Pollut. Bull. 127 (2018) 654–663, https://doi.org/10.1016/j.marpolbul.2017.12.055.
[44] S. Yeasmin, S. Karmaker, A.M. Rahman, M.M.M. Siraz, M.S. Sultana, Measurement of radioactvity in soil and vegetable samples in the northern area of Madhupur upzila at tangail district in Bangladesh and assessment of associated radological, Bangladesh, J. Phys. 16 (2014) 49–58.
[45] M. Sarker, M.M.M. Siraz, M. Jafor Dewan, S. Pervin, A.F.M. Mizanur Rahman, S. Yeasmin, Measurement of radioactivity for the assessment of radiological risk in sand sample collected from kuakata and cox ' s bazar sea beach located in measurement of radioactivity for the assessment of radiological risk in sand sample collected from kuakata an, Dhaka Univ. J. Appl. Sci. Eng. 6 (2021) 52–57.
[46] M.M.M. Siraz, S. Pervin, S. Banik, A.K.M.M. Rahman, A.F.M.M. Rahman,

S. Yeasmin, Estimation of radiation hazards from imported zirconium materials used in ceramic tiles industries in Bangladesh estimation of radiation hazards from imported zirconium materials used in ceramic tiles industries in Bangladesh, Nucl. Sci. Appl. 28 (1–2) (2020) 1–5.

[47] A. Sultana, M.M. Siraz, S. Pervin, A.M. Rahman, S.K. Das, S. Yeasmin, Assessment of radioactivity and radiological hazard of different food items collected from local market in Bangladesh, J. Bangladesh Acad. Sci. 43 (2020) 141–148, https://doi.org/10.3329/jbas.v43i2.45735.

[48] M.N. Aktar, S.K. Das, S. Yeasmin, M.M. Siraz, A.M. Rahman, Measurement of radioactivity and assessment of radiological hazard of tea samples collected from local market in Bangladesh, J. Bangladesh Acad. Sci. 42 (2018) 171–176, https://doi.org/10.3329/jbas.v42i2.40049.

[49] S. Yeasmin, M. Siraz, A. Faisal, S. Pervin, M.S. Sultana, Study of radioactivity in sand of a new beach zone at cox's bazar in the southern part of Bangladesh, in: Int. Conf. Phys. Sustain. Dev. Technol, 2015, pp. 91–96.

[50] M.A. Kobeissi, O. El-Samad, I. Rachidi, Health assessment of natural radioactivity and radon exhalation rate in granites used as buildingmaterials in Lebanon, Radiat. Protect. Dosim. 153 (2013) 342–351, https://doi.org/10.1093/rpd/ncs110.

[51] R. Ravisankar, J. Chandramohan, A. Chandrasekaran, J. Prince Prakash Jebakumar, I. Vijayalakshmi, P. Vijayagopal, B. Venkatraman, Assessments of radioactivity concentration of natural radionuclides and radiological hazard indices in sediment samples from the East coast of Tamilnadu, India with statistical approach, Mar. Pollut. Bull. 97 (2015) 419–430, https://doi.org/10.1016/j.marpolbul.2015.05.058.

[52] M.T. Kolo, S.A.B.A. Aziz, M.U. Khandaker, K. Asaduzzaman, Y.M. Amin, Evaluation of radiological risks due to natural radioactivity around Lynas Advanced Material Plant environment, Kuantan, Pahang, Malaysia, Environ. Sci. Pollut. Res. 22 (2015) 13127–13136, https://doi.org/10.1007/S11356-015-4577-5.

[53] Bangladesh Bureau of Statistics, Report on Agriculture and Rural Statistics 2018, 2019. Dhaka.

[54] R. Khan, M.S. Islam, A.R.M. Tareq, K. Naher, A.R.M.T. Islam, M.A. Habib, M.A.B. Siddique, M.A. Islam, S. Das, M.B. Rashid, A.K.M.A. Ullah, M.M.H. Miah, S.U. Masrura, M. Bodrud-Doza, M.R. Sarker, A.B.M. Badruzzaman, Distribution, sources and ecological risk of trace elements and polycyclic aromatic hydrocarbons in sediments from a polluted urban river in central Bangladesh, Environ. Nanotechnol. Monit. Manag. 14 (2020), https://doi.org/10.1016/j.enmm.2020.100318.

[55] M.A. Habib, T. Basuki, S. Miyashita, W. Bekelesi, S. Nakashima, K. Phoungthong, R. Khan, M.B. Rashid, A.R.M.T. Islam, K. Techato, Distribution of naturally occurring radionuclides in soil around a coal-based power plant and their potential radiological risk assessment, Radiochim. Acta 107 (2019) 243–259, https://doi.org/10.1515/ract-2018-3044.

[56] A. Faanu, O.K. Adukpo, L. Tettey-Larbi, H. Lawluvi, D.O. Kpeglo, E.O. Darko, G. Emi-Reynolds, R.A. Awudu, C. Kansaana, P.A. Amoah, A.O. Efa, A.D. Ibrahim, B. Agyeman, R. Kpodzro, L. Agyeman, Natural radioactivity levels in soils, rocks and water at a mining concession of Perseus gold mine and surrounding towns in Central Region of Ghana, SpringerPlus 5 (2016) 1–16, https://doi.org/10.1186/s40064-016-1716-5.

[57] D. Roy, M.M.M. Siraz, M.J. Dewan, S. Pervin, A.F.M.M. Rahman, M.U. Khandaker, S. Yeasmin, Assessment of terrestrial radionuclides in the sandy soil from Guliakhali beach area of Chattogram, Bangladesh, J. Radioanal. Nucl. Chem. 331 (2022) 1299–1307, https://doi.org/10.1007/s10967-022-08196-2.

[58] J.A. dos Santos Júnior, R. dos Santos Amaral, J.M. do Nascimento Santos, A.N.C. da Silva, L.A.V. Rojas, M.O. Milan, J. de Almeida Maciel Neto, J.D. Bezerra, E.E.N. De Araújo, Radioactive disequilibrium and dynamic of natural radionuclides in soils in the state of pernambuco—Brazil, Radiat. Protect. Dosim. 182 (2018) 448–458, https://doi.org/10.1093/rpd/ncy101.

[59] J. Al Mahmud, M.M.M. Siraz, M.S. Alam, S.C. Das, D.A. Bradley, M.U. Khandaker, S. Tokonami, A. Shelley, S. Yeasmin, A study into the long-overlooked carcinogenic radon in bottled water and deep well water in Dhaka, Bangladesh, Int. J. Environ. Anal. Chem. (2023) 1–13, https://doi.org/10.1080/03067319.2022.2163895.

[60] M.M.M. Siraz, D. Roy, M.J. Dewan, M.S. Alam, J. A M, M.B. Rashid, M.U. Khandaker, D.A. Bradley, S. Yeasmin, Vertical distributions of radionuclides along the tourist-attractive marayon tong hill in the bandarban district of Bangladesh, Environ. Monit. Assess. 195 (2023) 382, https://doi.org/10.1007/s10661-023-10921-7.

[61] C.M. Alonso-Hernández, A.L. Toledo-Sibello, A. Guillén-Arruebarrena, R. Sibello-Hernández, Y. Morera-Gómez, H.A. Cartas-Águila, Natural radioactivity and evaluation of radiation hazards in soils from granitoide-granite geological formation in Cuba, Radiat. Protect. Dosim. 184 (2019) 5–11, https://doi.org/10.1093/rpd/ncy178.

[62] E. Kapdan, N. Altinsoy, G. Karahan, A. Yuksel, Outdoor radioactivity and health risk assessment for capital city Ankara, Turkey, J. Radioanal. Nucl. Chem. 318 (2018) 1033–1042, https://doi.org/10.1007/s10967-018-6060-5.

[63] K. Manisa, M. Erdogan, A. Usluer, H. Cetinkaya, U. Isik, L. Sahin, V. Zedef, Assessment of natural radioactivity level of soil and water in the region of Çorlu (Turkey), J. Radioanal. Nucl. Chem. 329 (2021) 1213–1221, https://doi.org/10.1007/s10967-021-07906-6.

[64] K.U. Reddy, C. Ningappa, J. Sannappa, Natural radioactivity level in soils around Kolar Gold Fields, Kolar district, Karnataka, India, J. Radioanal. Nucl. Chem. 314 (2017) 2037–2045, https://doi.org/10.1007/s10967-017-5545-y.

[65] G. Sankaran Pillai, P. Shahul Hameed, S.M. Mazhar Nazeeb Khan, Natural radioactivity levels in the soils and human risk assessment in Tiruchirappalli district (Tamil Nadu, India), J. Radioanal. Nucl. Chem. 307 (2016) 1265–1277, https://doi.org/10.1007/s10967-015-4367-z.

[66] B. Jananee, A. Rajalakshmi, V. Thangam, K.M. Bharath, V. Sathish, Natural radioactivity in soils of Elephant hills, Tamilnadu, India, J. Radioanal. Nucl. Chem. 329 (2021) 1261–1268, https://doi.org/10.1007/s10967-021-07886-7.

[67] M.A.M. Uosif, Z.A. Alrowaili, R. Elsaman, A.M.A. Mostafa, Soil–soybean transfer factor of natural radionuclides in different soil textures and the assessment of committed effective dose, Radiat. Protect. Dosim. 188 (2020) 529–535, https://doi.org/10.1093/rpd/ncaa005.

[68] M.A. Haydar, M.M. Hasan, I. Jahan, K. Fatema, M.I. Ali, D. Paul, M.U. Khandaker, The status of NORMs in natural environment adjacent to the Rooppur nuclear power plant of Bangladesh, Nucl. Eng. Technol. 53 (2021) 4114–4121, https://doi.org/10.1016/j.net.2021.06.025.

[69] M.J. Abedin, M.R. Karim, M.U. Khandaker, M. Kamal, S. Hossain, M.H.A. Miah, D.A. Bradley, M.R.I. Faruque, M.I. Sayyed, Dispersion of radionuclides from coal-fired brick kilns and concomitant impact on human health and the environment, Radiat. Phys. Chem. 177 (2020), 109165, https://doi.org/10.1016/j.radphyschem.2020.109165.

[70] N. Absar, J. Abedin, M.M. Rahman, M.H. Miah, N. Siddique, M. Kamal, M.I. Chowdhury, A.A.M. Sulieman, M.R.I. Faruque, M.U. Khandaker, D.A. Bradley, A. Alsubaie, Radionuclides transfer from soil to tea leaves and estimation of committed effective dose to the Bangladesh populace, Life 11 (2021) 1–15, https://doi.org/10.3390/life11040282.

[71] M. Dhingra, M. Kumar, R. Mehra, N. Sharma, Assessment of primordial radionuclide contents in soil samples and of impact of coal-based thermal power plant: a study in Tarn Taran district in Punjab, India, Radiat. Protect. Environ. 43 (2020) 49, https://doi.org/10.4103/rpe.rpe_11_20.

[72] G. Liu, Q. Luo, M. Ding, J. Feng, Natural radionuclides in soil near a coal-fired power plant in the high background radiation area, South China, Environ. Monit. Assess. 187 (2015), https://doi.org/10.1007/s10661-015-4501-y.

[73] Z. Papp, Z. Dezso, S. Daróczy, Significant radioactive contamination of soil around a coal-fired thermal power plant, J. Environ. Radioact. 59 (2002) 191–205, https://doi.org/10.1016/S0265-931X(01)00071-6.

[74] F. Gür, G. Yaprak, Natural radionuclide emission from coal-fired power plants in the southwestern of Turkey and the population exposure to external radiation in their vicinity, J. Environ. Sci. Heal. - Part A Toxic/Hazardous Subst. Environ. Eng. 45 (2010) 1900–1908, https://doi.org/10.1080/10934529.2010.520608.

[75] H. Aytekin, R. Baldik, On the radiological character of a coal-fired power plant at the town of Çatalağzi, Turkey, Turkish, J. Eng. Environ. Sci. 32 (2008) 101–105.

[76] A.K. Mahur, M. Gupta, R. Varshney, R.G. Sonkawade, K.D. Verma, R. Prasad, Radon exhalation and gamma radioactivity levels in soil and radiation hazard assessment in the surrounding area of National Thermal Power Corporation, Dadri (U.P.), India, Radiat. Meas. 50 (2013) 130–135, https://doi.org/10.1016/j.radmeas.2012.09.008.

[77] E. Charro, R. Pardo, V. Peña, Statistical analysis of the spatial distribution of radionuclides in soils around a coal-fired power plant in Spain, J. Environ. Radioact. 124 (2013) 84–92, https://doi.org/10.1016/j.jenvrad.2013.04.011.

[78] H. Bem, P. Wieczorkowski, M. Budzanowski, Evaluation of technologically enhanced natural radiation near the coal-fired power plants in the Lodz region of Poland, J. Environ. Radioact. 61 (2002) 191–201, https://doi.org/10.1016/S0265-931X(01)00126-6.

[79] L. Wang, X. Lu, Natural radionuclide concentrations in soils around Baoji coal-fired power plant, China, Radiat. Eff. Defect Solid 162 (2007) 677–683, https://doi.org/10.1080/10420150601143153.

[80] X. Lu, C. Zhao, C. Chen, W. Liu, Radioactivity level of soil around Baqiao coal-fired power plant in China, Radiat. Phys. Chem. 81 (2012) 1827–1832, https://doi.org/10.1016/j.radphyschem.2012.07.013.

[81] NEA-OECD, Exposure to Radiation from Natural Radioactivity in Building Materials, Report by NEA group of Experts, OECD, Paris, France, 1979.